THE ROYAL INSTITUTION OF NAVAL ARCHITECTS

ISSUED FOR WRITTEN DISCUSSION

bij 159
W7(1970)

Contributions to the discussion of this paper are invited; they should be typewritten and should reach the Secretary, The Royal Institution of Naval Architects, 10 Upper Belgrave Street, London, S.W.1. not later than 29th January, 1971.

The Institution is not, as a body, responsible for the statements made nor for the opinions expressed by individual authors.

Large-Deflexion Behaviour of Ship Plate Panels Under Normal Pressure and In-Plane Loading

by B. Aalami, Ph.D.* and J. C. Chapman, Ph.D.† (Member)

SUMMARY: A finite difference analysis has been used to study the effects of loading, initial deformation and boundary restraints, on the behaviour of square and rectangular plates. It is concluded that when initial deformation is taken into account membrane stresses can have a significant effect on the behaviour of plates of practical dimensions. Depending on the magnitude and shape of the deformation, the in-plane stiffness may be reduced by as much as 30%. The stress distribution is shown to be greatly affected by the extensional as well as the flexural boundary conditions. Some biaxial thrust cases are considered; the results throw some light on the behaviour of bottom plating and illustrate the well known advantage of longitudinal framing.

NOTATION

x, y, z	Rectangular coordinates
u, v, w	Total displacement of mid-surface of plate in x, y and z directions caused by the applied loading
w_o	Initial deformation of plate corresponding to w
h	Plate thickness
σ_x, σ_y	Stresses in x and y directions respectively (suffices b and m to be added for bending and membrane stresses)
σ_{xy}	Shear stress in xy plane
ν	Poisson's ratio
∇^4	$= \partial^4/\partial x^4 + 2\partial^4/\partial x^2\partial y^2 + \partial^4/\partial y^4$

1. INTRODUCTION

Ref. (1) presented a large deflexion finite difference analysis of orthotropic plates under normal loading. The edges of the plate were assumed not to deflect, whilst elastic edge restraints were provided against rotational, extensional and tengential movements. The effect of continuity over the edge supports can be taken into account by allotting values to these restraints. The effects of membrane stresses and boundary restraints were studied and the results were presented in a systematic non-dimensional form. It was found, not unexpectedly, that the extensional boundary conditions had a major influence on the magnitude of the membrane stresses and hence on the deflexions and surface stresses.

Ref. (2) extended the analysis to include externally applied in-plane forces, to account for boundary conditions related to individual plates within a symmetrical array of plating under loading, and to allow for sinking of the edges and for unfairness of the plating. It was found that unfairness can have a major influence on the behaviour of the plate under in-plane load. The limits of applicability of the small deflexion theory [3] were explored and it was shown that within the range of practical plate dimensions it was necessary to consider large deflexion effects in order to obtain a sufficiently accurate expression of plate behaviour.

The purpose of this paper is to illustrate the behaviour of plates having proportions, loading and boundary conditions encountered in ships. Particular attention is directed towards the influence of unfairness and the effectiveness of the plating as part of a structure subjected to in-plane loading in one or two directions. Thus the analysis is a necessary prelude to the elastic analysis of the complete structure. It also takes the local analysis to the point where an elasto-plastic treatment must begin.

2. CONTINUITY

Plate panels do not act in isolation. Together with their adjacent panels, they form a structural system which sustains the applied loading. The continuity of each panel is achieved through the restraints exerted on it by the surrounding structural components.

The restraint of the adjacent structure at the boundary of a panel of plating may be rotational, normal to plane of the plate, extensional (in the plane of plate and perpendicular to the boundary) and tangential (in the plane of plate and parallel to the boundary). The first two are flexural and the other two are membrane conditions. The nature and magnitudes of these restraints depend on the loading as well as the geometry of the adjoining structural components. A full account of the influence of each of the above types of restraint on the behaviour of an isolated panel is given in Refs. [3] and [2].

For bottom shell plates which are surrounded by indentical panels, the rotation of the boundaries in respect of uniform normal loading is zero, due to symmetry, and the isolated panel may be treated as rotationally fixed. Initial out of flatness and in-plane loading, however, may result in rotations at the boundaries, in which case the rotational restraint of the supporting stiffener of web is mobilised. Stiffeners with large torsional rigidity (including angles, due to the effect of the flange) result in a condition close to full fixity of the edges [4].

The sides of the panels supported on stiffeners sink under transverse pressure, due to flexibility of stiffeners in the normal plane. The bending of stiffeners in double bottoms however is usually restricted by strutting against the tank top, and the stiffener deflexion is small compared to the plate deflexion. To limit the number of variables in this presentation, the edge deflexion has been taken as zero.

The panels of plating forming the ship's bottom structure may by symmetry be assumed to remain rectangular under load—that is, the panel sides change in length but remain straight.

* Associate Professor at Aria-Mehr University of Technology, Tehran.
† Reader in Structural Engineering, Imperial College, London.

Moreover, from equilibrium considerations (assuming the tangential edge shear to be zero) the total extensional force on each edge must equal the applied in-plane loading. The above condition is between the extremes that the edges are fully free (zero membrane normal stress), and that the edges are fully fixed at the boundaries against extensional displacements. Other membrane boundary conditions will prevail under unsymmetrical loading conditions.

In the solutions given, the tangential edge forces have been taken as zero. This is a correct assumption in respect of a symmetrically deformed connected array of panels and is also correct in respect of antisymmetrically deformed panels under in-plane loading only. There will however be shear forces (arising from membrane displacements) between the plate and supporting stiffener, and these have not been taken into account in this presentation, but the program does allow a finite tangential restraint to be considered.

3. LOADING

(i) Transverse (normal) pressure: Outer shell panels are subjected to almost uniform hydrostatic still water pressure of the order 10-20 lb/sq. in., which may be increased several times due to dynamic effects. For the tank top and deck panels, the normal loading is due to cargo and fork lift trucks, and may be concentrated. The use of a graded mesh, which the program permits, is particularly beneficial in respect of patch loading.

(ii) In-plane loading due to bending of the double-bottom: The double-bottom structure spans transversely and longitudinally between the sides of the ship and transverse bulkheads and the plate panels are therefore subjected to biaxial edge thrusts. The relative magnitudes of the thrusts depend on the position of the panel and on the side ratio of the double-bottom. The panel edge stress due to bending at the centre of a double-bottom structure may be of the order of 5 tons/sq. in.

(iii) In-plane loading due to longitudinal hull bending: The total longitudinal bending stress for mild steel may be of the order of 8 tons/sq. in. This must be added to the stresses due to (i) and (ii).

4. UNFAIRNESS OF PLATING

Unfairness due to fabrication or due to permanent set as a result of loading, results in a loss of stiffness against in-plane loading. The effect of unfairness may well be greater than the effect of transverse pressure, and should therefore be taken into account in the analysis.

5. LOSS OF PLATE STIFFNESSES

A plate under combined loading undergoes changes in its flexural and in-plane stiffnesses due to the interaction of bending and membrane phenomena, and the changes are more pronounced for thinner plates and higher values of loading. For ship plate dimensions and loading, the changes can be significant.

(i) Flexural stiffness: End-thrust reduces the flexural rigidity of the plate. The flexural stiffness for a flat plate approaches zero as in-plane loading reaches the critical buckling load of a plate. For a plate subjected to an end-thrust $\frac{1}{4}$ of its buckling load, the reduction is about 33% [5],[3].

(ii) On the other hand, transverse deflexion of the plate due to pressure or due to unfairness results in the development of membrane stresses which increase the flexural stiffness of the plate.

(iii) In-plane stiffness: the loss of in-plane stiffness is due either to the shear lag phenomenon, which is not the subject of discussion of this paper, or to out of plane deflexion, of the plate. Due to out of plane deflexion, the plate's stiffness against in-plane loading is reduced. The 'buckling breadth ratio' concept is used to measure this loss of stiffness.

The definition of buckling breadth ratio may be based on either a strain or a stress criterion. The distinction is necessitated by the existence of biaxial stresses and non-zero values of Poissons's ratio. The buckling breadth ratio based on strains is defined as the ratio of flat plate strain to the actual overall strain of the plate, and can be used to estimate the deformation of the structure of which the plate is a part.

The buckling breadth ratio based on stresses, is the ratio of average membrane direct stress normal to the edge to the maximum direct membrane stress developed in the same direction. This ratio enables the stresses in the structure to be calculated.

6. METHOD OF ANALYSIS

The large deflexion elastic behaviour of plates can be expressed by two simultaneous partial differential equations (see Appendix). The equations, together with the boundary conditions (both flexural and membrane) are expressed in terms of finite differences and programmed for computer. Graded meshes are used to improve the accuracy of the results[3].

7. PRESENTATION OF RESULTS

For the results given in this paper, the flexural boundary conditions are assumed either rotationally free or rotationally fixed. The membrane boundary conditions are:

(i) zero membrane direct stress and zero membrane shear stress

Symbol	Flexural boundary conditions
——	rigidly supported, rotationally free
═══	rigidly supported, rotationally fixed

(i)

Symbol	Membrane boundary conditions and in-plane loading
——	zero direct stress, zero shear stress
▽—▽	zero extensional displacement, zero shear stress
═══	edge remains straight, zero average direct stress, zero shear stress
□□□	uniform extensional displacement, specified average direct stress, zero shear stress

(ii)

Fig. 1. Symbolic representation of boundaries and in-plane loading

(ii) edges remain straight (sum of direct membrane stress equal to applied edge thrust) and zero membrane shear stress

(iii) edges fixed against normal extensional displacement and zero shear stress.

The above boundary conditions are listed symbolically in Fig. 1. At the corner of each graphical figure, the relevant boundary conditions are shown by means of two rectangles; the first rectangle bearing the cartesian coordinates relates to flexural boundary conditions, and the second rectangle indicates the membrane boundary conditions.

For each case, centre line deflected profiles, bending moment and membrane stress distributions are shown graphically. Central deflexions, and the magnitude of bending moments and membrane stresses are tabulated in a non-dimensional form.

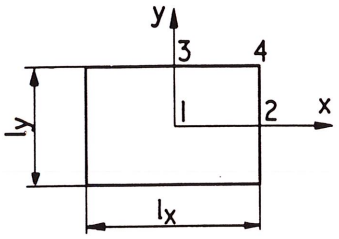

Fig. 2. Coordinate system

Plate	Boundary conditions: Flexural	Membrane	w_o/h	$l_x^4 q/h^4 E$	Loading description	Mesh	Table
1			0	yes	increasing transverse pressure	12 × 20 graded No 2	1-3
2			0	yes	increasing transverse pressure	12 × 20 graded No 1	1-3
3			0	yes	increasing transverse pressure	12 × 20 graded No 2	1-3
4			0	yes	increasing transverse pressure	12 × 20 graded No 1	1,2,4
5			0	yes	increasing transverse pressure	12 × 20 graded No 1	1,2,4,17
6			0	yes	increasing transverse pressure	12 × 20 graded No 1	1,2,4
7			0	2	Increasing Nx	12 × 12 graded No 3	5,7
8			0	10			
9			0	2	Increasing Ny	12 × 12 graded No 1	6,8
10			0	10			6,8,17
11			0	20			6,8

Fig. 3 (i). Summary of solutions presented

The non-dimensional coefficients are based on a value of Poisson's ratio $\nu = 0{\cdot}3$, and the non-dimensionalisation procedures (which are formulated to embrace orthotropic plates) are outlined in Ref. (2).

Surface stresses at certain points may be calculated as the sum of appropriate membrane and bending stresses obtainable from the coefficients given in the Tables.

The relationship between the non-dimensional coefficients and plate deflexion and stresses are as follows:

$$\frac{w}{h} = W/3{\cdot}305 \qquad \frac{l_x^2 M_x}{EH^4} = M'_x/36{\cdot}09$$

$$\frac{l_x^2 \sigma_{xm}}{h^2 E} = N'_x/10{\cdot}92$$

$$\frac{l_x^2 M_y}{Eh^4} = M'_y/36{\cdot}09$$

$$\frac{l_x^2 \sigma_{ym}}{h^2 E} = N'_y/10{\cdot}92$$

Where necessary, a numerical suffix is used to indicate the location in the plate to which the quantities refer. Those locations are numbered in Fig. 2.

The solutions discussed in this paper are listed in Fig. 3, in which the boundary conditions, initial unfairness, the type of loading, the mesh used in the analysis, and the corresponding Table of non-dimensional results, are given.

In order to illustrate the significance of results, each solution is followed by numerical examples. The examples mostly refer to 30 x 90 in. rectangular plates (shorter side assumed along x-axis), with $E = 30 \times 10^6$ lb./sq. in. and $\nu = 0{\cdot}3$. Two plate thicknesses are considered, 0·5 in. and 0·35 in.

Plate	Boundary conditions: Flexural	Membrane	w_o/h	$l_x^4 q/h^4 E$	Loading description	Mesh	Table
12			0·1	0	Increasing Nx	12 × 12 uniform	9-10
13			0·5	0			
14			1·0	0			
15			0·1	0	Increasing Nx	12 × 12 graded No. 3	11-12
16			0·5	0			
17			1·0	0			
18			0·05	0	Increasing Ny	12 × 20 graded No. 1	13-14
19			0·1	0			
20			0·5	0			15,17
21			1·0	0			
22			0·5	0	Nx = Ny Increasing end-thrusts	12 × 20 graded No. 1	15
23			0·5	0	Nx = 0·5 Ny Increasing end-thrusts	12 × 20 graded No. 1	13
24			0·5	0	Increasing Ny	12 × 20 graded No. 1	15-16
25			0·5	0	Nx = Ny Increasing end-thrusts	12 × 20 graded No. 1	15-16
26			0·5	0	Nx = 0·5 Ny Increasing end-thrusts	12 × 20 graded No. 1	
27			0·5	10	Increasing Ny	12 × 20 graded No. 1	17

Fig. 3 (ii). Summary of solutions presented

8. SOLUTIONS

8.1 3/1 Rectangular plates under uniform transverse pressure (Plates 1-6, Figs. 4-7, Tables 1-4)

Selected results are given for both rotationally free and rotationally fixed plates, each with three different membrane boundary conditions. The membrane boundary conditions are:

(i) edges are free from normal stress and membrane shear stress, corresponding to a freely supported isolated plate (Plates 1 and 4)

(ii) edges are free to translate while remaining straight, with total normal force on each edge equal to zero; the membrane boundary shear stresses are assumed zero. These conditions approximate to those of individual plates in a symmetrical array of panels under transverse pressure (Plates 2 and 5)

(iii) edges are fully fixed against translation with membrane shear stress equal to zero (Plates 3 and 6). In this case the solution is practically indistinguishable from that for zero tangential displacement [3].

It can be seen from Figs. 4 and 5, that for both rotationally free and rotationally fixed plates, membrane stresses result in a reduction of curvature at the centre of the plate, particularly in the longitudinal direction. In rotationally free plates, maximum bending stress occurs at the centre in the transverse direction. In the longitudinal direction maximum bending stress occurs near the shorter edges, but its value is less than the maximum in the transverse direction. In rotationally fixed plates, maximum bending stress is at the mid-point of either the shorter or longer edges.

The distributions of membrane stress for the limiting membrane boundary conditions (Plates 1, 3, 4 and 6) are shown in Figs. 6 and 7. For plates with fixed membrane boundary conditions, membrane stresses do not vary over the central region of the plate, where the plate behaves as part of a long plate strip.

The range of loading covered in the tabulated results is sufficient to reach the elastic limit for most practical ship plates. The principal values of deflexion and stress for 0·5 in. plates and 0·35 in. plates under transverse pressures of 23·2 and 11 lb/sq. in. respectively are given in examples 1 and 2. For both examples, a marked deviation is observed between the linear and the non-linear results for rotationally free plates. In Example 1 (Table 1) membrane stresses developed are generally much less than the bending stresses, but their effect on bending stresses is nevertheless very marked. For example, in the rotationally free case, the linear solution gives a bending stress at the centre of plate $\sigma_{xb} = 26{\cdot}4$ tons/sq. in., whereas membrane restraints can reduce the bending stress to 12·0 tons/sq. in. (Plate 3). The rotationally fixed plates, under the same transverse pressure and the same membrane boundary conditions are not affected to the same extent by membrane effects, as may be noted in both examples 1 and 2. This is because the flexural resistance is greater for clamped edges.

Non-linear results for Plates 1-6 are given in Tables 3 and 4 in a non-dimensional form, from which deflexion and stresses for other plate thicknesses and values of transverse pressure may be calculated. At the bottom of each table linear solutions are also given.

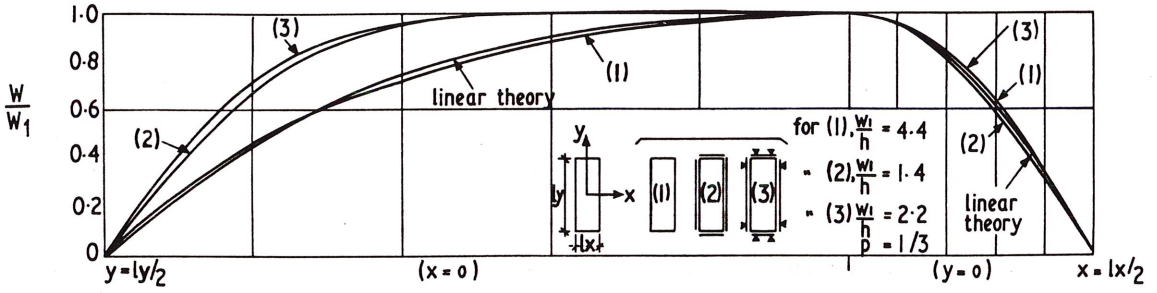

(i) Deflexion profiles along the centre lines

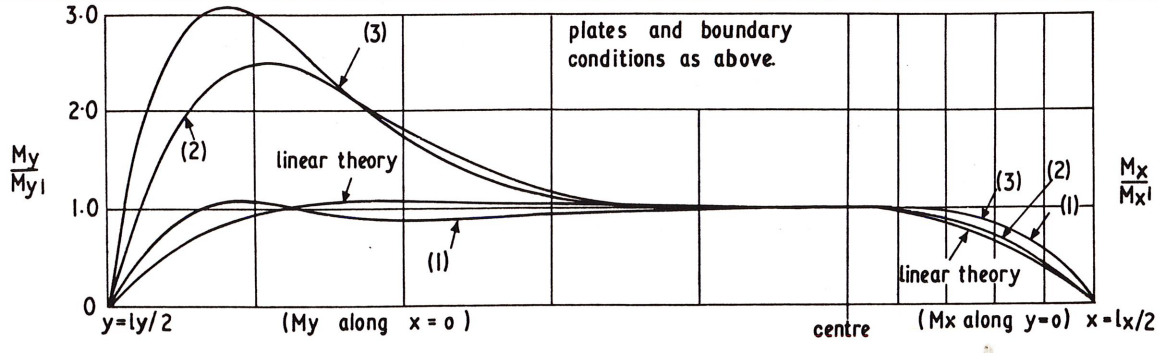

(ii) Bending moment profiles along the centre lines

Fig. 4. Rotationally free rectangular plate under uniform transverse pressure (Plates 1-3)

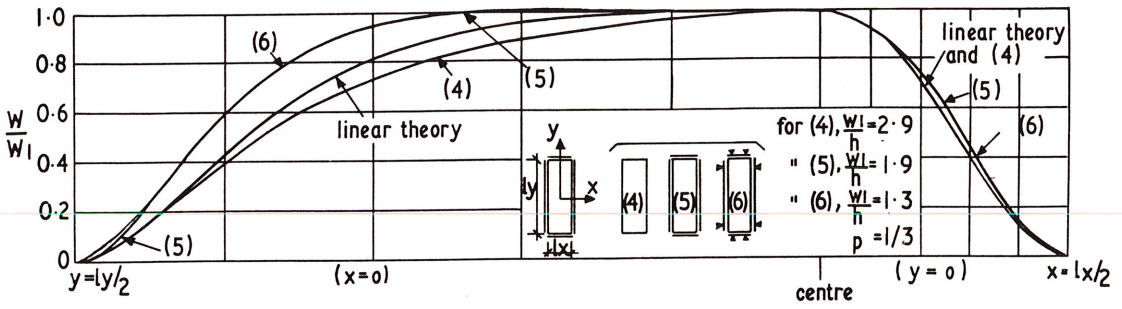

(i) Deflexion profiles along the centre lines

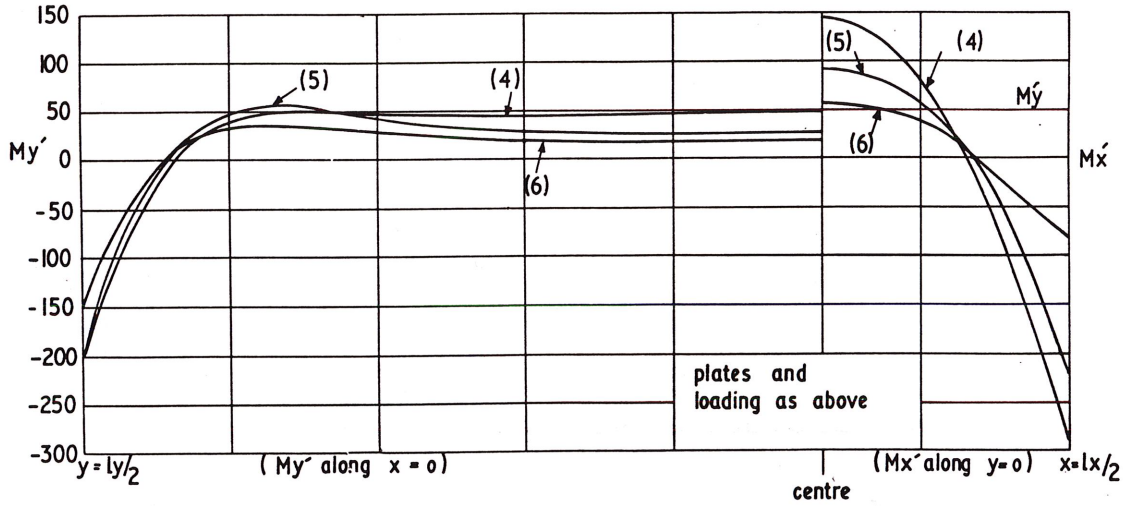

(ii) Bending moment profiles along the centre lines

Fig. 5. Rotationally fixed rectangular plates under uniform transverse pressure (Plates 4-6, $l_x^4 q/h^4 E$ = 96·98).

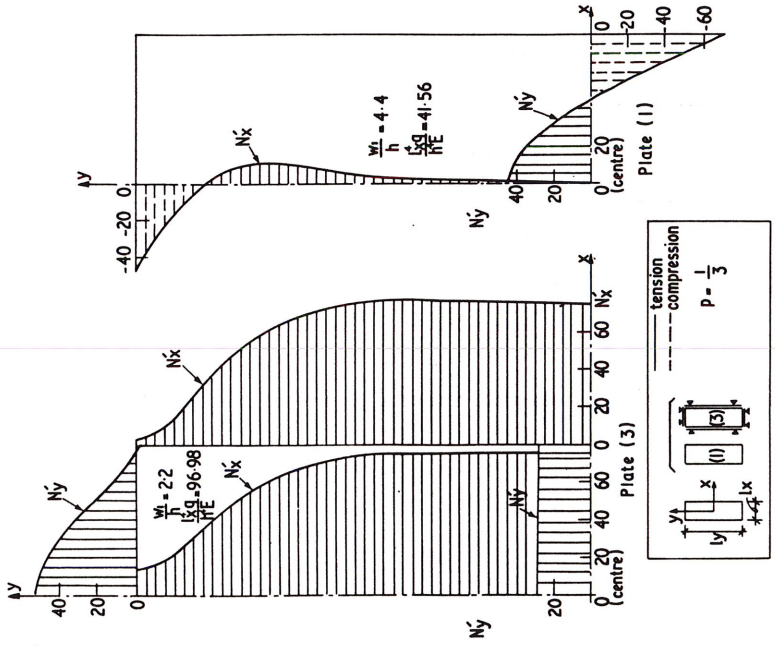

Fig. 6. Rotationally free rectangular plate under uniform transverse pressure. Distribution of membrane stress along the centre lines (Plates 1, 3).

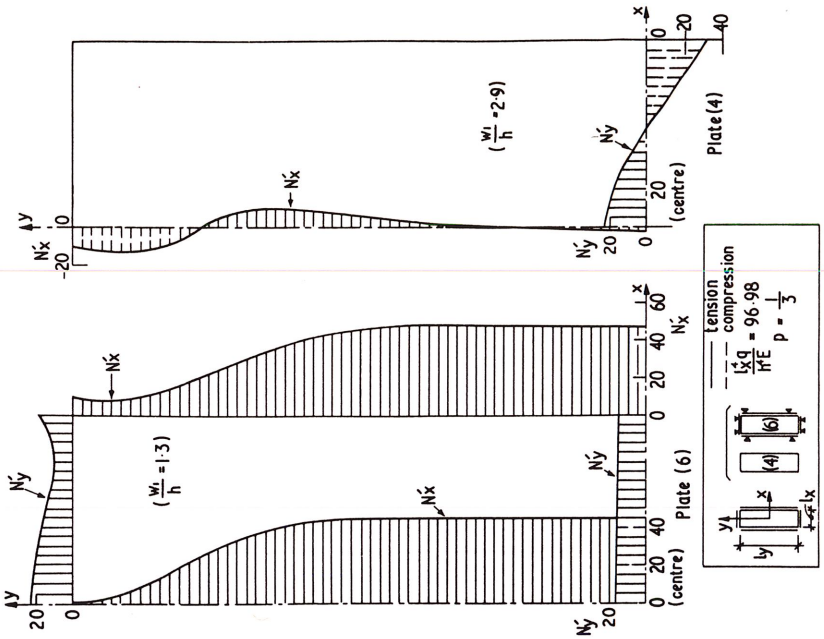

Fig. 7. Rotationally fixed rectangular plates under uniform transverse pressure. Bending moment profiles along the centre lines (Plates 4, 6).

8.2 Rotationally fixed plates under constant uniform transverse pressure and increasing uniaxial end-thrust (Plates 7-11, Figs, 8-12, Tables 5-8)

The plates are subjected to a constant uniform transverse pressure and an increasing end-thrust. The average value of the end-thrust is increased to the critical buckling load of the plate in ten steps. All the edges remain straight throughout the loading, with the average value of the in-plane direct stress on the unloaded edges equal to zero. These boundary conditions approximate the conditions of an individual plate panel of a ship hull, subjected to transverse water pressure and to uniaxial end-thrust due to the overall bending of the ship.

Results for square plates ($l_x^4q/Eh^4 = 2, 10$) and for 3/1 rectangular plates ($l_x^4q/Eh^4 = 2, 10, 20$) are given in Figs, 8-12 and in Tables 5 and 6.

Figs. 8 and 9 show the variation of transverse deflexion with increasing average end-thrust, and Fig. 10 (i) shows the deflexion profiles along the longitudinal centre line for three values of end-thrust. As the magnitude of end-thrust increases the deflected profile of the plate approaches the shape of its incipient buckling mode. For $l_x^4q/Eh^4 = 2$, at a value of end-thrust close to the critical load, the central deflexion of the plate moves above the line of support despite the action of transverse pressure. This suggests that for incomplete rotational restraints the adjacent plate panels may not deflect symmetrically.

In Fig. 10 (ii), the distribution of bending moment along the longitudinal centre line is shown for $l_x^4q/Eh^4 = 2$. As may be noted from the figure, the distribution is very sensitive to the magnitude of end-thrust, and the position and magnitude of the maximum moment in the longitudinal direction cannot, in this case, be estimated from the linearised solution [5].

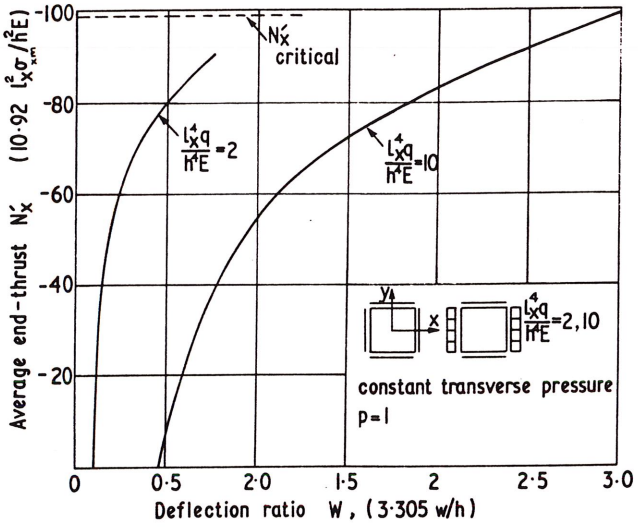

Fig. 8. Rotationally fixed square plate under uniform transverse pressure and end-thrust. Deflexion at centre (Plates 7, 8).

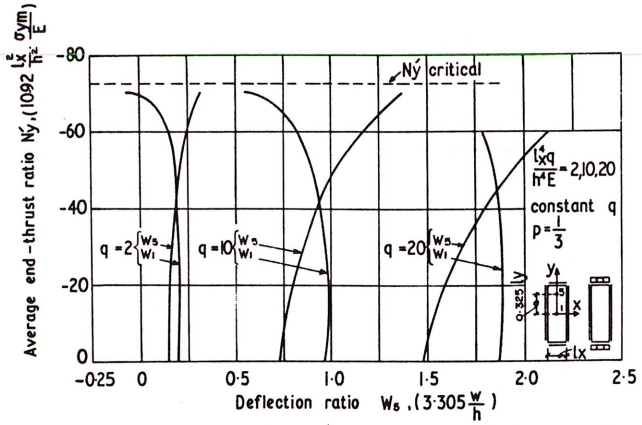

Fig. 9. Rotationally fixed rectangular plate under transverse pressure and end-thrust. Deflexions at centre and at x = 0, y = 0·325 *ly* (Plates 9-11).

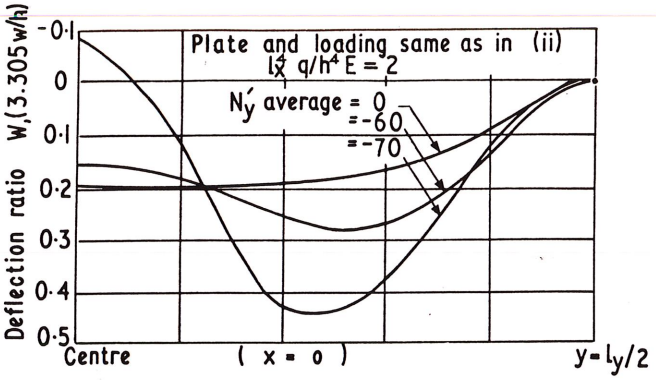

(i) Deflexion profiles along y-y centre line

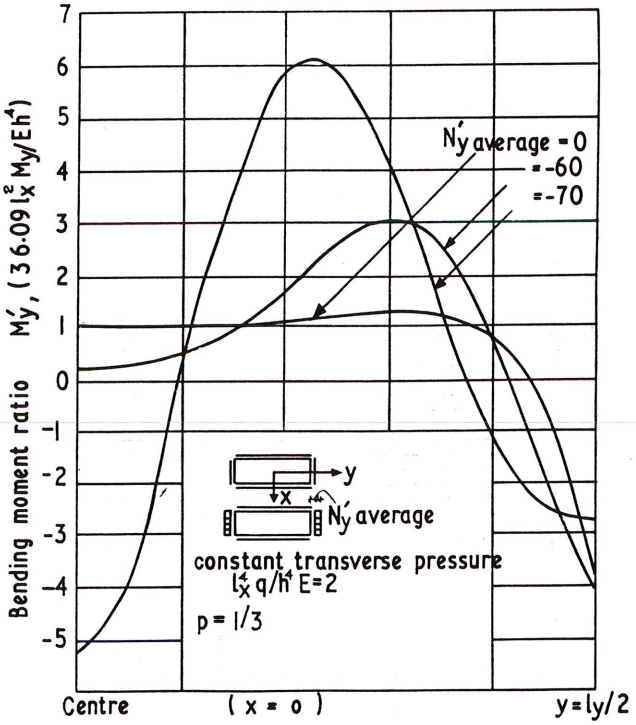

(ii) Bending moment profiles along y-y centre line

Fig. 10. Rotationally fixed plate under normal transverse pressure and increasing end-thrust (Plates 9-11)

For square plates, the bending moment profiles are shown in Fig. 11 and the distribution of membrane stress along the centre lines in Fig. 12. The change observed in the distribution of membrane stress is small, and this is also true for other plates of this group, for which no figures are given. Consequently there is little loss in the in-plane load carrying capacity of the plates, and this is also indicated by the buckling breadth ratios given in Tables 5 and 6.

Numerical examples are given in Tables 7 and 8 for square and and rectangular plates with h = 0·5 and 0·35 in. The maximum deviation in membrane stress distribution from the straight line does not exceed 8%.

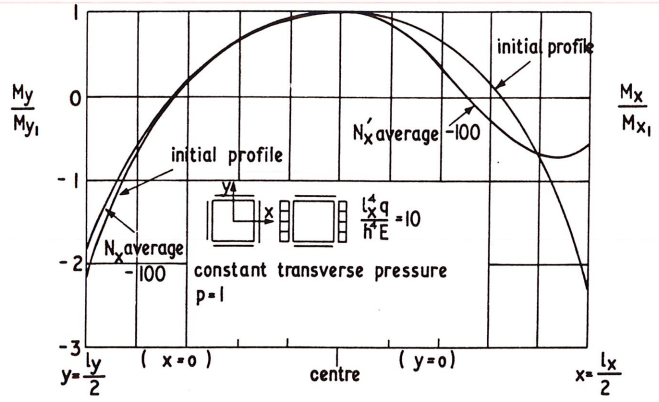

Fig. 11. Rotationally fixed square plate under uniform transverse pressure and end-thrust. Bending moment profiles along the centre lines

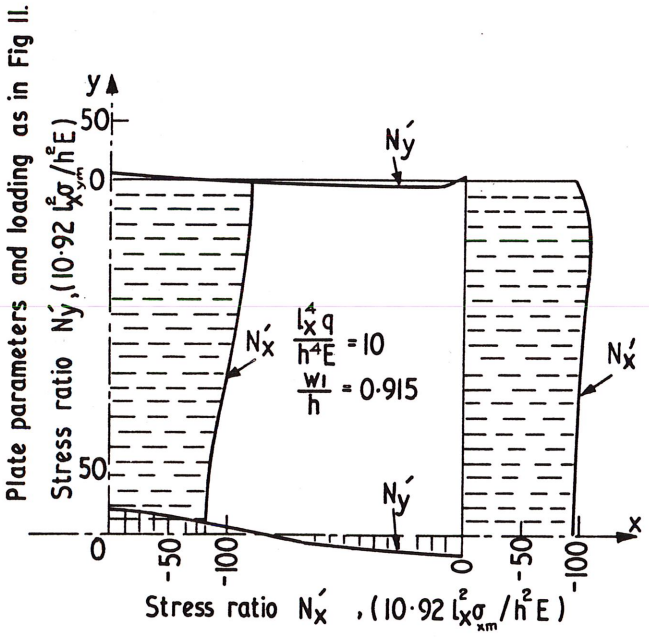

Fig. 12. Rotationally fixed square plate under uniform transverse pressure and end-thrust. Distribution of membrane stress (Plates 7, 8, $N'_x = -100$)

8.3 Initially deformed rotationally free square plates under increasing end-thrust (Plates 12-14, Figs. 13-16, Tables 9-10)

The rotationally free flexural boundary condition corresponds to the case when adjacent panels deflect freely in opposite directions under the in-plane loading. The membrane boundary conditions are the same as in the previous case.

The initial deformations of the plates are assumed to be in the form of a half sine wave along both axes with the maximum central deflexion w_{01}/h = 0·1, 0·5 and 1 respectively. In each case the average end-thrust is raised from zero to its maximum value in seven steps.

Fig. 13 shows the variation of the total central deflexion with the average end-thrust. According to the linearised theory the deflexion for w_{01}/h = 1 would be 10 times the deflexion for W_{01}/h = 0·1 for all values of thrust, whereas the non-linear solution shows that N'_x = 30, for example, the deflexion ratio is about 4. insert (at)

For the highest values of end-thrust plotted, the bending moment profiles along the centre lines are shown in Fig. 14. The position of maximum bending moment (initially at the centre) gradually moves towards the sides as the end-thrust increases. For the value of loading shown in Fig. 14, the maximum bending moment for w_{01}/h = 1 is at the quarter length of the plate and its magnitude is 15% more than the central value.

The distribution of membrane stress for the same load is shown in Fig. 15. The variation across the plate of the longi-

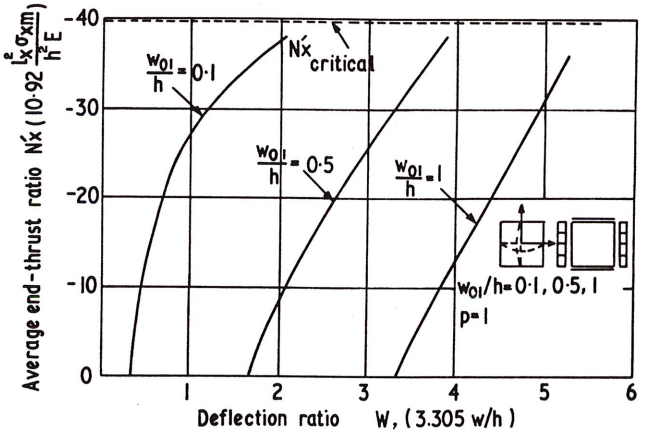

Fig. 13. Rotationally free initially deformed square plate under end-thrust. Deflexion at centre (Plates 12-14).

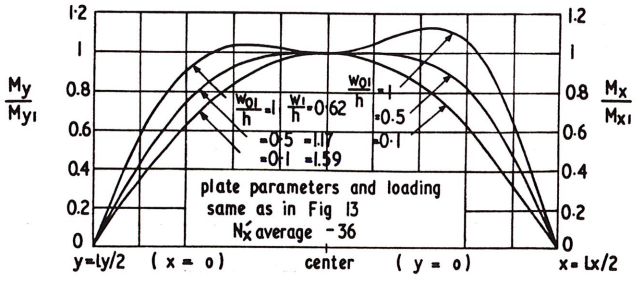

Fig. 14. Rotationally free initially deformed plate under end-thrust. Bending moment profiles along the centre lines (Plates 12-14).

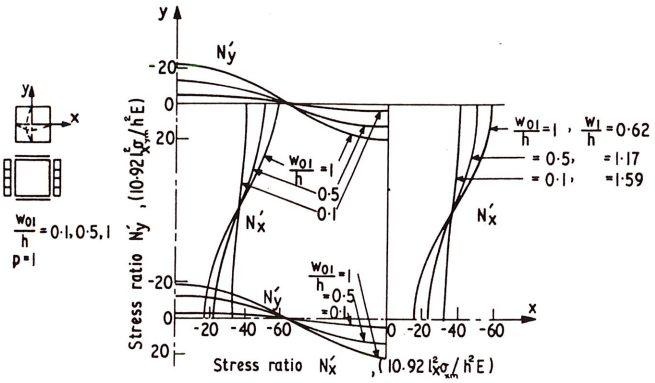

Fig. 15. Rotationally free initially deformed plates under end-thrust. Distribution of membrane stress

(Plates 12-14, $N'_x = -36$)

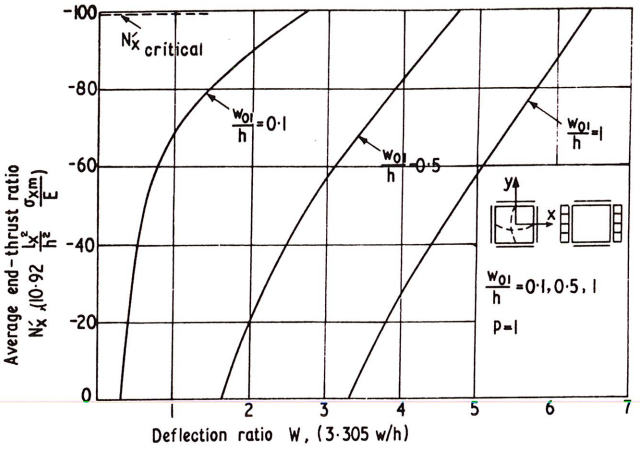

Fig. 17. Initially deformed rotationally fixed plates under end-thrust. Deflexion at centre. (Plates 15-17).

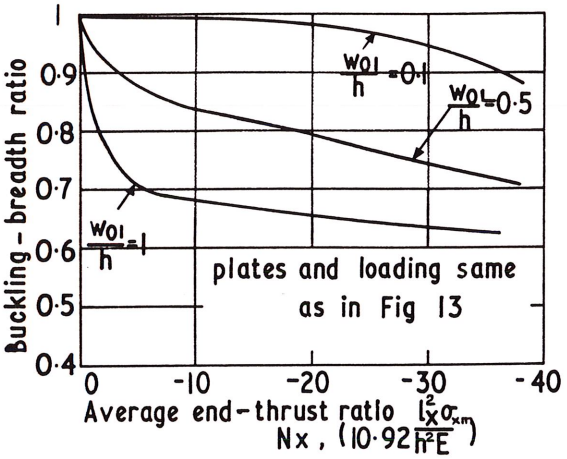

Fig. 16. Rotationally free initially deformed plates under end-thrust. Variation of buckling breadth ratio with average end-thrust (Plates 12-14)

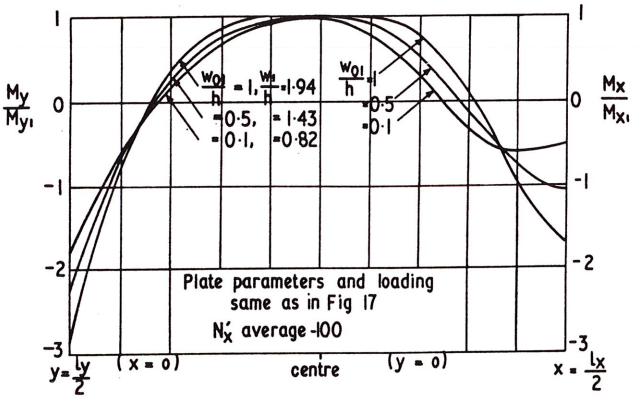

Fig. 18. Rotationally fixed initially deformed plates under end-thrust. Bending moment profiles along the centre lines (Plates 15-17).

tudinal stress can be clearly seen. Buckling breadth ratios based on stress or strain are found to be almost the same. The variation of the ratio (based on stress) with increasing end-thrust is shown in Fig. 16. At the critical buckling load, the buckling breadth ratio for the plate with $w_{01}/h = 1$ is about 2/3.

Numerical examples are given in Table 9 for a 0·5 in. plate subjected to an end-thrust of 12·28 tons/sq. in. (93% of its critical value) with three different values of initial deformation.

It is noted that the bending stress (and also the additional central deflexion of the plate) for $w_{01}/h = 0{\cdot}05$ is larger than for $w_{01}/h = 1$, contrary to what would be expected from the linearised theory. The bending stresses developed at the centre are of the same order as the applied in-plane stresses, and do not vary in proportion to the initial deformation.

8.4 Initially deformed rotationally fixed square plates under increasing end-thrust (Plates 15-17, Figs. 17-20, Tables 11-12

As in the previous case, the plates are assumed to have an initial deformation in the form of a half sine wave with $w_{01}/h = 0{\cdot}1$, 0·5 and 1·0. The end-thrust is gradually increased to the critical value.

In this case maximum positive bending moment occurs at the centre of the plate in the direction of applied loading. The maximum negative moment occurs at the mid-point of the unloaded edges in the transverse direction (Table 12), the latter being the greatest bending moment in the plate. The distribution of bending moment along the centre lines is shown by the profiles given in Fig. 18 for the maximum value of end-thrust reached.

The distribution of membrane stress for the maximum loading is shown in Fig. 19. In this case buckling breadth ratios based on stress and strain have different values, the former being consistently lower than the latter (Fig. 20). This difference is due to the variation in longitudinal edge stress (and strain) along the plate.

Numerical examples are given for plates 15-17 in Table 11. The 0·5 in. plate is subjected to an end-thrust of 12·28 tons/sq. in. equal to 38% of its critical buckling value and the 0·35 in. plate is acted upon by an end-thrust of 11·7 tons/sq. in. equal to 72% of its critical value. Again the bending stresses are not proportional to the initial deformation. The buckling breadth ratio (based on stress) for $w_{01}/h = 1$ is 0·77 for the 0·5 in. plate and 0·72 for the 0·35 in. plate.

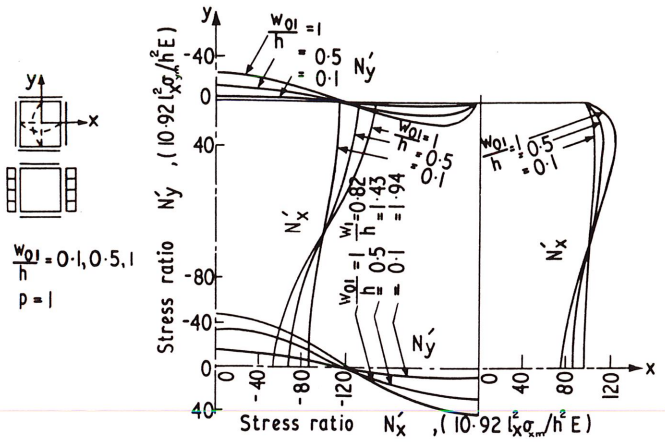

Fig. 19. Rotationally fixed initially deformed plates under end-thrust. Distribution of membrane stress (Plates 15-17, $N'_x = -100$).

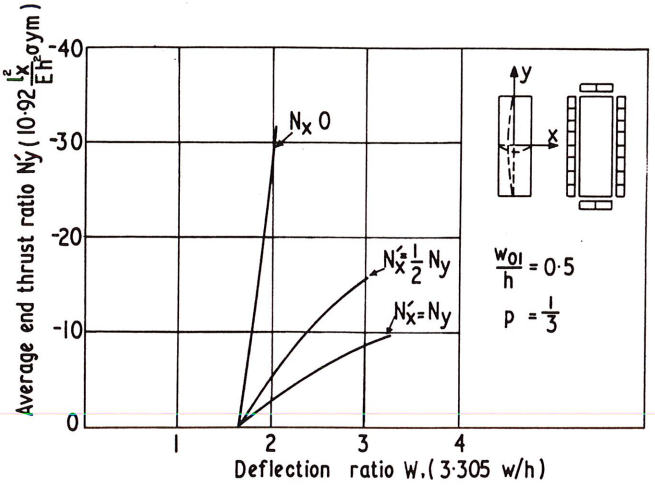

Fig. 21. Initially deformed rotationally fixed rectangular plate under end-thrust. Deflexion at centre (Plates 20, 22, 23, $w_{01}/h = 0{\cdot}5$).

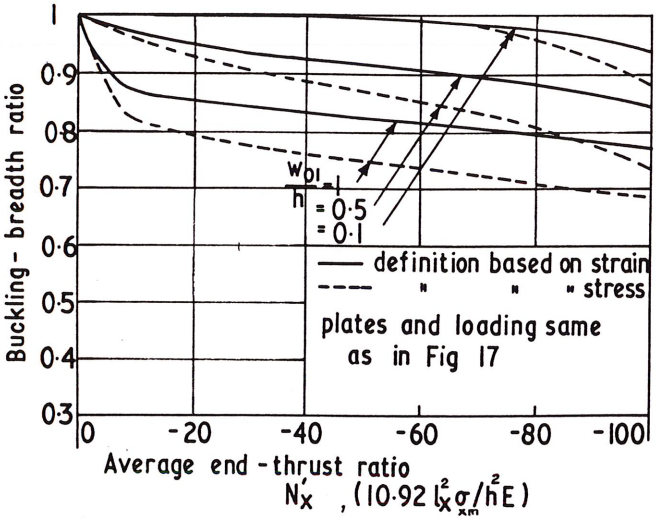

Fig. 20. Rotationally fixed initially deformed plates under end-thrust. Variation of buckling breadth ratio with average end-thrust (Plates 15-17).

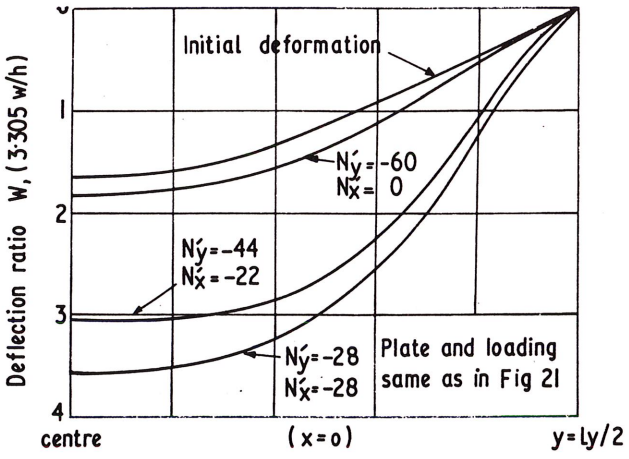

Fig. 22. Initially deformed rotationally fixed rectangular plate under end-thrust. Deflexion profiles along Y-Y centre line (Plates 20, 22, 23, $w_{01}/h = 0{\cdot}5$).

8.5 Initially deformed rotationally fixed 3/1 rectangular plates under uniaxial end-thrust (Plates 18-21, Figs. 21-24, Tables 13-14)

Four plates with initial deformations in the form of a half sine wave, $w_{01}/h = 0{\cdot}05, 0{\cdot}1, 0{\cdot}5$ and $1{\cdot}0$ are considered. The membrane boundary conditions, as in plate 5, correspond to single panels in an array of plates under symmetrical conditions. The plates are loaded uniaxially along the longitudinal axis with an increasing end-thrust.

For the case of $w_{01}/h = 0{\cdot}5$, the variation with end-thrust of central deflexion and deflected profile, and the bending moment distribution, are shown in Figs. 21 and 23. Deflexion profiles for this and other loading cases are plotted in Fig. 29.

The net deflexion of plates with small values of unfairness ($w_{01}/h = 0{\cdot}05, 0{\cdot}1$) is close to three half waves (the incipient buckling mode), whereas for larger values of unfairness ($w_{01}/h = 0{\cdot}5, 1$) the initial one half wave profile becomes dominant and is magnified under increasing end-thrust.

Maximum bending moment occurs in the transverse direction at mid-point of the unloaded edges. In the longitudinal direction, the position of maximum moment depends upon the loading, and as may be noted from Fig. 23, its position changes between the centre and the end of the plate. For a given value of in-plane loading, plates having greater initial deformation develop higher bending stresses, but the relative increase is less than the increase in initial deformation.

The in-plane load carrying capacity of the plates, characterised by the buckling breadth ratio is practically $1{\cdot}0$ for $w_{01}/h = 0{\cdot}05$ and $0{\cdot}1$, and is decreased up to 1% for higher values of w_{01}/h (Table 13), whereas square plates with the same type of loading and initial deformation show appreciable loss in buckling breadth. This is because a single half wave has been assumed for the initial deformed shape of the rectangular plate.

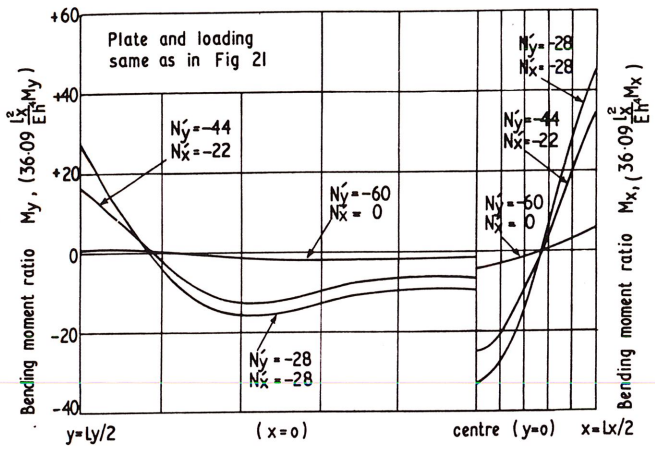

Fig. 23. Initially deformed rotationally fixed plate under end-thrust. Bending moment profiles along the centre lines (Plates 20, 22, 23, $w_{01}/h = 0{\cdot}5$).

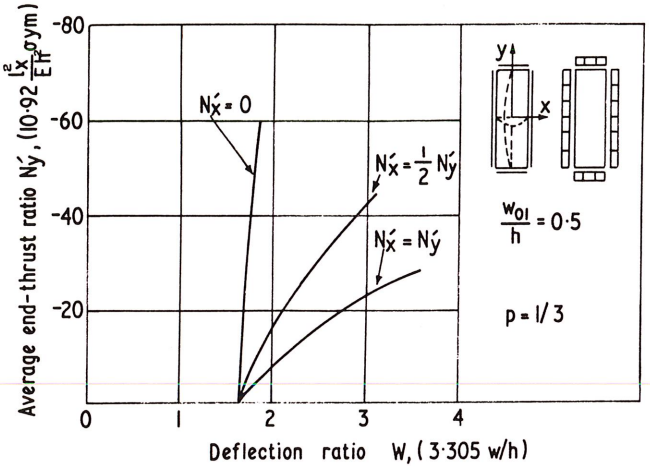

Fig. 25. Initially deformed rotationally free rectangular plate under end-thrust. Deflexion at centre (Plates 24-26, $w_{01}/h = 0{\cdot}5$).

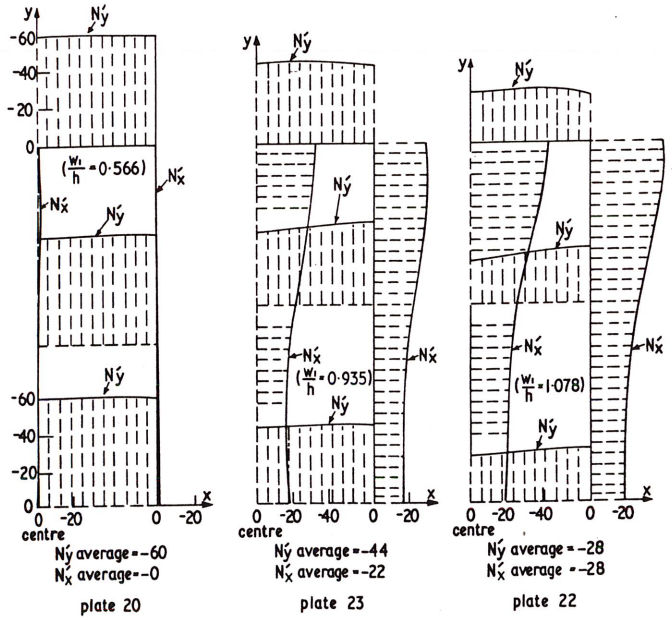

Fig. 24. Initially deformed rotationally fixed rectangular plate under end-thrust. Distribution of membrane stress along the centre lines (Plates 20, 22, 23, $w_{01}/h = 0{\cdot}5$).

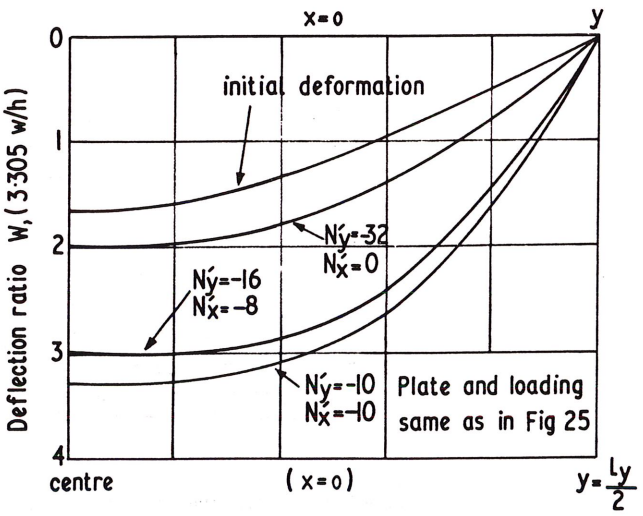

Fig. 26. Initially deformed rotationally free rectangular plate under end-thrust. Deflexion profiles along Y-Y axis (Plates 24-26, $w_{01}/h = 0{\cdot}5$).

Numerical examples are given in Table 14 for plates 19-21, in which an 0·5 in. plate is subjected to an end-thrust of 13·6 tons/sq. in (equal to 59% of the critical buckling value), and an 0·35 in. plate is subjected to an end-thrust of 10 tons/sq. in. (equal to 78% of the critical value).

8.6 Initially deformed 3/1 rectangular plates under biaxial edge thrust (Plates 22-26, Figs. 25-28, Tables 15-16)

The plates are assumed to have an initial out of flatness in the form of a half sine wave with maximum deflexion at centre equal to half the plate thickness.

The following three cases of end-thrust are considered:

(i) uniaxial longitudinal end-thrust (Plates 20 and 24),

(ii) equal biaxial edge-thrust (Plates 22 and 25),

(iii) biaxial edge-thrust, with the longitudinal stress twice the transverse stress (Plates 23 and 26).

For each type of loading, rotationally fixed and rotationally free edges are considered, with membrane boundary conditions as in Plate 2.

Variations of central deflexion with increasing end-thrust, deflexion profiles, bending moment distribution and membrane stress distribution are shown for the rotationally fixed plates in Figs. 21-24, and for the rotationally free plates in Figs. 25-28.

As may be expected, in-plane loading in the transverse direction causes larger bending stresses in the plate than loading in

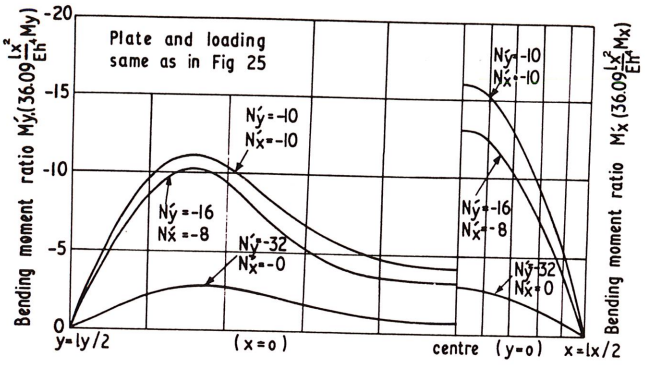

Fig. 27. Initially deformed rotationally free rectangular plate under end-thrust. Bending moment profiles along the centre lines

Plates 24-26, $w_{o1}/h = 0{\cdot}5$).

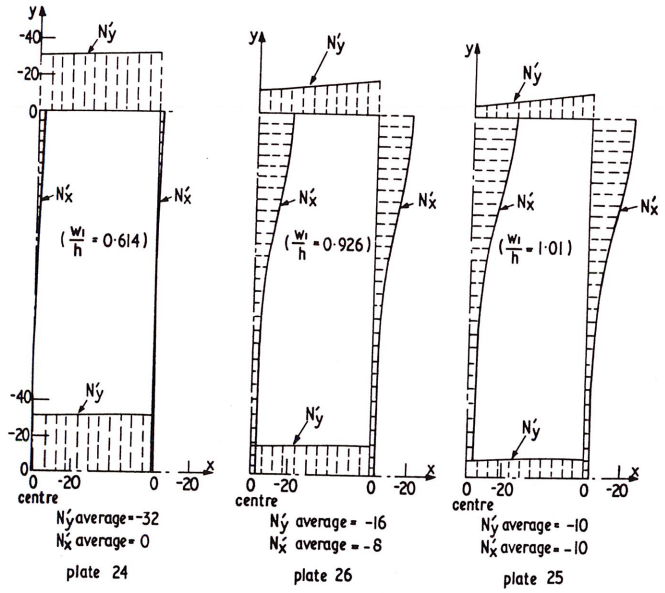

Fig. 28. Initially deformed rotationally free rectangular plate under end-thrust. Distribution of membrane stress along the centre lines (Plates 24-26, $w_{o1}/h = 0{\cdot}5$).

the longitudinal direction (Table 15). Also the buckling breadths are much less in respect of transverse in-plane loading. These differences illustrate the advantage of longitudinal framing. It can also be seen that the transverse loading affects the buckling breadth in the longitudinal direction.

8.7 Initially deformed 3/1 rectangular plate under combined action of end-thrust and transverse pressure (Plate 27, Fig. 29, Table 17)

The boundary conditions of the plate are the same as for Plate 5. The initial deformation is in the form of a half sine wave with $w_{o1}/h = 0{\cdot}5$. The transverse pressure is uniformly distributed and the end-thrust is applied along the longitudinal axis.

A solution for the same plate with initial deformation and end-thrust (Plate 20), and another solution with end-thrust and transverse pressure (Plate 10) are discussed previously.

In Fig. 29 deflexion profiles for various cases are compiled for comparison. The arrow at the top right hand corner of each graph represents the end-thrust, and transverse pressure, if present, is shown on the uppermost line of each figure.

To illustrate the effects of combined loading, numerical examples are given for 0·5 in. plate and 0·35 in. plate. In each case deflexions and stresses for four loading conditions are calculated and listed together in Table 17.

The loading cases for the 0·5 in. plate are (i) q = 23·2 lb/sq. in. alone, (ii) q = 23·2 lb/sq. in. together with σ_{ym} average = 12·28 tons/sq. in., (iii) $w_{o1}/h = 0{\cdot}5$ with σ_{ym} average = 12·28 tons/sq. in., (iv) $w_{o1}/h = 0{\cdot}5$ with q = 23·2 lb/sq. in. and σ_{ym} average = 12·28 tons/sq. in. Similar loading conditions are used for the 0·35 in. plate.

In both examples it can be seen that the membrane stresses due to end-thrust are not affected appreciably by initial deformation and transverse pressure. High bending stresses are developed, due to transverse pressure alone; the addition of end-thrust, as may be seen again, does not necessarily magnify the existing bending stresses as inferred from linear theories. Under the combined action of end-thrust and transverse pressure, the stresses developed in an initially deformed plate are generally less than the sum of stresses due to individual actions of transverse pressure on flat plate alone, and an end-thrust acting on the initially deformed plate. Bending stresses at the mid-point of the loaded edges are an exception to this, but they are not the highest bending stresses in the plate.

9. CONCLUSIONS

From the analysis of results it is concluded that the plates considered undergo elastic deformations large enough for the effects of membrane action to become significant, and a large deflexion solution must be used for a proper estimate of stresses and deflexions. The importance of the membrane effect depends on the membrane as well as the flexural boundary conditions.

Transverse pressure

For plates under transverse pressure and uniaxial end-thrust, the values of transverse pressures considered are not high enough to affect the distribution pattern of membrane stresses significantly, and the loss in in-plane stiffness of such plates is negligible (Examples 3 and 4).

Unfairness of plating

For square plates with initial deformations of the order of plate thickness, the unfairness of plating results in extensive changes in the distribution of membrane stress, and also results in development of flexural stresses of the same order of magnitude as membrane stresses. There is a significant loss of in-plane stiffness, which may amount to about 30% under working conditions (Examples 5 and 6).

For 3/1 rectangular plates under end-thrust and with maximum initial deformations up to plate thickness, the loss in longitudinal stiffness is not significant if the unfairness is in the form of one-half wave along the longitudinal axis. The same order of loss in longitudinal stiffness as in square plates, may be expected if the unfairness is in three-half waves. The transverse stiffness will however be considerably reduced by a single half wave deformation.

For a given value of longitudinal end-thrust, plates having greater initial deformations develop higher bending stresses, but the proportional increase in bending stresses is less than the increase in initial deformation. The difference is not reflected by the linearised solution and is large enough to justify the use of a large deflexion solution.

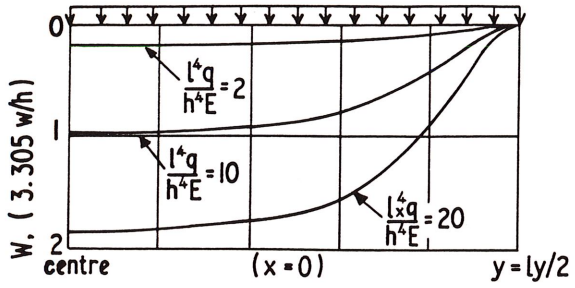

(i) Initially flat plate under transverse pressure alone ($N'_y = O = N'_x$, plate 5)

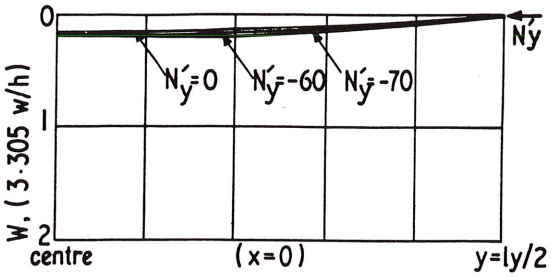

(ii) Initially deformed plate under in-plane loading alone $\left(\frac{W_o}{h} = 0{\cdot}05, \frac{l_x^4 q}{h^4 E} = O,$ plate 18$\right)$

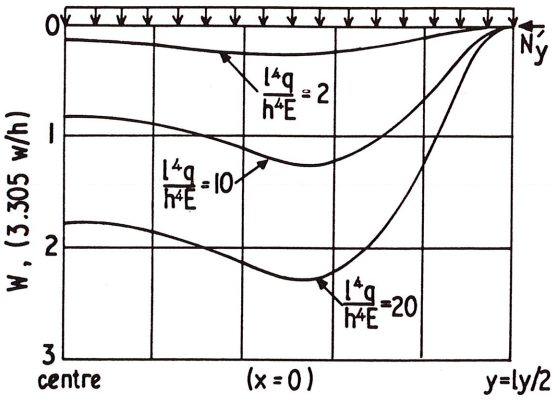

(iii) Initially flat plate under transverse pressure and in-plane loading

(N_y average = –60, $N'_x = O$, plate 9-11)

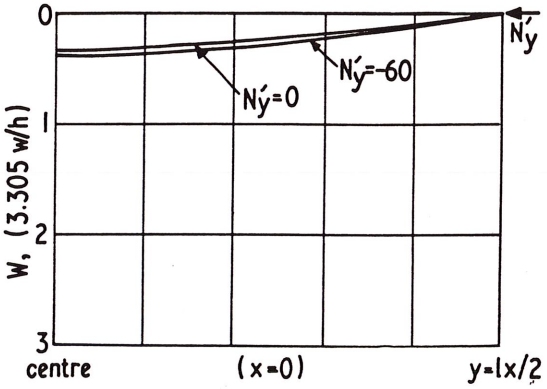

(iv) Initially deformed plate under in-plane loading alone $\left(\frac{W_o}{h} = 0{\cdot}1, \frac{l_x^4 q}{h^4 E} = O,$ plate 19$\right)$

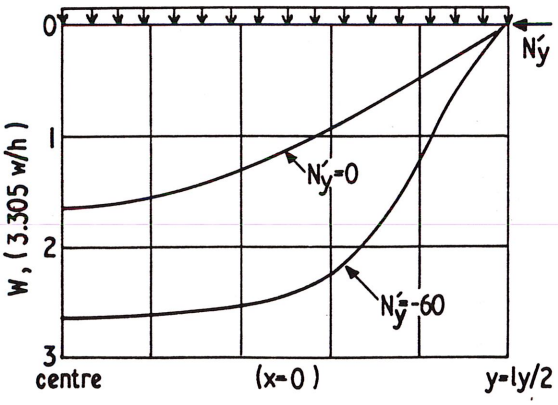

(v) Initially deformed plate under transverse pressure and in-plane loading

$\left(\frac{W_o}{h} = 0{\cdot}5, \frac{l_x^4 q}{h^4 E} = 10,$ plate 27$\right)$

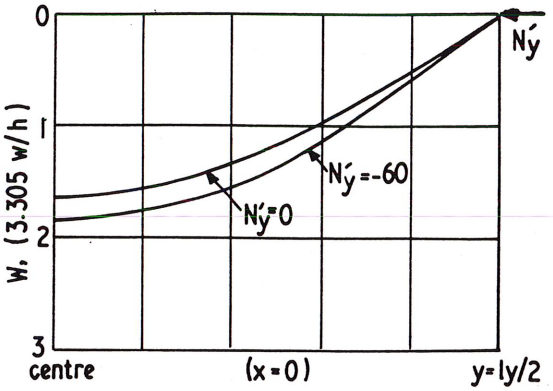

(vi) Initially deformed plate under in-plane loading alone $\left(\frac{W_o}{h} = 0{\cdot}5, \frac{l_x^4 q}{h^4 E} = O,$ plate 20$\right)$

Fig. 29. Rotationally fixed rectangular plates under various loading conditions. Deflexion profiles along Y-Y axis.

Biaxial stresses

Compressive loading on the longer sides of a rectangular plate is much more detrimental to plate behaviour than the same loading on the shorter sides. It follows that the plating should be framed in the direction of the primary loading. The effect of biaxial loading on rectangular plates is illustrated in the examples.

Initially deformed plates under combined action of transverse pressure and end-thrust

It is shown in the case considered that a conservative estimate of stresses due to combined load can be obtained by adding the stresses due to transverse pressure on a flat plate, to the stresses due to in-plane loading on the initially deformed plate.

APPENDIX

The large deflexion behaviour of initially deformed plates (Fig. 2) can be expressed in terms of the two following fourth order simultaneous partial differential equations[6,7].

$$\nabla^4 w = \frac{q}{D} + \left(\frac{\partial^2 f}{\partial y^2}\cdot\frac{\partial^2 w}{\partial x^2} - \frac{\partial^2 f}{\partial x \partial y}\cdot\frac{\partial^2 w}{\partial x \partial y} + \frac{\partial^2 f}{\partial x^2}\cdot\frac{\partial^2 w}{\partial y^2}\right) + \nabla^4 w_o \quad (1)$$

$$\nabla^4 f = Eh\left\{\left(\frac{\partial^2 w}{\partial x \partial y}\right)^2 - \frac{\partial^2 w}{\partial x^2}\cdot\frac{\partial^2 w}{\partial y^2}\right\} \quad (2)$$

The equations are expressed in terms of plate deflexion (w), and Airy's stress function (f) defined such that

$$\sigma_{xm} h = \frac{\partial^2 f}{\partial y^2},\quad \sigma_{ym} h = \frac{\partial^2 f}{\partial x^2},\quad \sigma_{xy} h = -\frac{\partial^2 f}{\partial x \partial y} \quad (3)$$

All the other quantities related to the bending and membrane actions of the plate can be expressed in terms of the two variables w and f.

The boundary conditions of the cases described in this paper are as follows:

For bending action:

(i) at $x = l_x/2$ and $y = l_y/2$ $\quad w = 0$ (4)

(ii) for simply supported plates

at $x = l_x/2$ $\quad \partial^2 w/\partial x^2 = 0$ (5)

at $y = l_y/2$ $\quad \partial^2 w/\partial y^2 = 0$ (6) and

for clamped (rotationally fixed) plates

at $x = l_x/2$ $\quad \partial w/\partial x = 0$ (7)

at $y = l_y/2$ $\quad \partial w/\partial y = 0$ (8)

For membrane action

(iii) at $x = l_x/2$ and $y = l_y/2$ $\sigma_{xy} = 0$ and in terms of f $\quad \partial^2 f/\partial y \partial x = 0$ (9)

(iv) for the applied loading

at $x = l_x/2$

$$u = \frac{1}{Eh}\int_0^{l_x/2}\left(\frac{\partial^2 f}{\partial y^2} - \nu\frac{\partial^2 f}{\partial x^2}\right)dx - \frac{1}{2}\int_0^{l_x/2}\left(\frac{\partial w}{\partial x}\right)^2 dx +$$

$$\frac{1}{2}\int_0^{l_x/2}\left(\frac{\partial w_o}{\partial x}\right)^2 dx = \text{constant} \quad (10)$$

$$2\int_0^{l'_y/2}\sigma_{xm}\cdot h\,dy = 2\int_0^{l_y/2}\frac{\partial^2 f}{\partial y^2}\,dy =$$

l_y(average applied in-plane stress) (11)

and at $y = l_y/2$

$$v = \frac{1}{Eh}\int_0^{l_y/2}\left(\frac{\partial^2 f}{\partial x^2} - \nu\frac{\partial^2 f}{\partial y^2}\right)dx - \int_0^{l_y/2}\left(\frac{\partial w}{\partial y}\right)^2 dx +$$

$$\frac{1}{2}\int_0^{l_y/2}\left(\frac{\partial w_o}{\partial y}\right)^2 dx = \text{constant} \quad (12)$$

$$2\int_0^{l_x/2}\sigma_{ym}\cdot h\,dx = 2\int_0^{l_x/2}\frac{\partial^2 f}{\partial x^2}\,dx =$$

l_x(average applied in-plane stress) (13)

In the expressions (11) and (13) above, if the edges are unloaded the average applied in-plane stress is specified as zero.

The graded meshes used for the problems discussed in this paper are given in Table 18.

11. ACKNOWLEDGEMENT

The work described formed part of a programme of research undertaken for The British Ship Research Association.

The authors are indebted to Mr. M. J. Niayesh of Aria-Mehr University of Technology, Tehran, for preparing graphs and tables, and to Mr. M. Zahedi of Imperial College for checking and correcting the manuscript, graphs and tables.

12. REFERENCES

1. Basu, A. K. and Chapman, J. C.: 'Large Deflexion Behaviour of Transversely Loaded Rectangular Orthotropic Plates'. (Proc. Inst. Civil Engineers, Sept. 1966), Vol. 35.
2. Aalami, B. and Chapman, J. C.: 'Large Deflexion Behaviour of Rectangular Orthotropic Plates under Transverse and In-plane Loads'. (Proc. Inst. Civil Engineers, March 1969).
3. Aalami, B.: 'Non-linear Behaviour of Rectangular Orthotropic Plates under Transverse and In-plane Loads'. (Ph.D. Thesis, University of London, 1967).
4. Williams, D. G.: 'Analysis of a Doubly Plated Grillage under In-plane and Normal loading'. (Ph.D. Thesis, University of London, 1969).
5. Bleich, J. F.: 'Buckling Strength of Metal Structures'. (McGraw Hill Book Co., London, 1952).
6. Von Karman, T.: 'Festigkeitsprobleme in Maschinenbau Encyklopaedie der Mathematischen Wissenschaften, 1910), IV.
7. Marguerre, K.: 'Zur Theorie der Gekruemmter Platte Grosser Formaendenung'. (Proc. Fifth Int. Cong. Appl. Mech., Cambridge, 1938).

TABLE 1 Example 1 3/1 rectangular plate under uniform transverse pressure, h = 0·5 in., q = 23·2 lb/sq. in.

	Central deflexion in.	Bending stresses tons/sq.in.				Membrane stresses tons/sq.in.					
		σ_{xb1}	σ_{xb2}	σ_{yb1}	σ_{yb3}	σ_{xm1}	σ_{ym1}	σ_{xm2}	σ_{ym2}	σ_{xm3}	σ_{ym3}
Linear	0·670	±26·4	0	±9·05	0	0	0	0	0	0	0
Plate 1	0·655	±25·9	0	±9·09	0	−0·069	1·35	0	−2·13	−1·24	0
Plate 2	0·456	±17.55	0	±5·23	0	1·98	0·074	2·08	−0·097	−5·38	1·73
Plate 3	0·315	±12·0	0	±3·68	0	4·09	1·34	4·13	1·24	0·463	2·08
Linear	0·148	±9·41	±18·5	±2·88	±12·9	0	0	0	0	0	0
Plate 4	0·149	±9·46	±18·6	±2·90	±12·9	−0·032	0·056	0	−0·070	−0·052	0
Plate 5	0·146	±9·26	±18·4	±2·81	±13·02	0·225	0·027	0·244	−0·195	−0·518	0·034
Plate 6	0·141	±8·83	±17·9	±2·68	±12·76	0·727	0·231	0·745	0·186	0·003	0·240

TABLE 2 Example 2 3/1 rectangular plate under uniform transverse pressure, h = 0·35 in., q = 11 lb/sq.in.

	Central deflexion in.	Bending stresses tons/sq.in.				Membrane stresses tons/sq.in.					
		σ_{xb1}	σ_{xb2}	σ_{yb1}	σ_{yb3}	σ_{xm1}	σ_{ym1}	σ_{xm2}	σ_{ym2}	σ_{xm3}	σ_{ym3}
Linear	0·938	±25·8	0	±8·85	0	0	0	0	0	0	0
Plate 1	0·867	±23·9	0	±8·51	0	−0·028	2·30	0	−3·68	−2·17	0
Plate 2	0·481	±12·8	0	±3·79	0	1·76	0·027	1·85	−0·067	−6·30	2·55
Plate 3	0·303	±7·90	0	±2·37	0	3·72	1·28	3·75	1·22	0·480	2·12
Linear	0·209	±9·22	±18·1	±2·81	±12·66	0	0	0	0	0	0
Plate 4	0·209	±9·26	±18·2	±2·86	±12·65	−0·053	0·113	0	−0·142	−0·094	0
Plate 5	0·197	±8·65	±17·5	±2·61	±12·89	0·38	0·043	0·42	−0·028	−0·96	0·071
Plate 6	0·178	±7·64	±16·3	±2·30	±12·02	1·09	0·458	1·12	0·295	0·003	0·380

TABLE 3 Rotationally free 3/1 rectangular plates under uniform transverse pressure

Plate	$\frac{l_x^4}{h^4} \cdot \frac{q}{E}$	W_1	M'_{X1}	M'_{Y1}	N'_{Y1}	N'_{y2}	N'_{X1}	N'_{X2}	N'_{X3}	N'_{y3}
1	4·156	1.84	17·8	6·12	0·631	−0·983	−0·078	0	−0·611	0
	20·78	8·51	82·1	29·3	14·7	−23·5	−0·166	0	−13·9	0
	41·56	14·7	139	49·6	44·1	−71·6	0·936	0	−46·7	0
2	2	0·847	8·17	2·73	0·053	−0·057	0·687	0·702	−1·12	0·233
	10	3·01	28·4	8·46	0·217	−0·285	5·83	6·10	−15·8	5·06
	20	4·55	42·5	12·5	0·170	−0·405	10·5	11·1	−37·8	15·3
3	20·78	2·92	26·6	7·98	8·03	7·63	23·2	23·4	3·03	13·3
	41·56	3·82	34·1	10·1	14·6	14·1	40·3	40·6	6·09	25·5
	63·73	4·46	39·2	11·7	20·8	20·1	55·7	56·2	9·18	37·1
	96·98	5·18	44·9	13·4	28·8	28·0	75·7	76·3	13·5	52·6
(linear)		1.23	1.19	4·07						
$36·09 \frac{l_x^4}{h^4} \cdot \frac{q}{E} = 2 \times 10^{-2}$		$\times 10^{-1}$	$\times 10^{-2}$	0	0	0	0	0	0	

TABLE 4 Rotationally fixed 3/1 rectangular plates under uniform transverse pressure

Plate	$\frac{l_x^4}{h^4}\cdot\frac{q}{E}$	W_1	M'_{x1}	M_{y1}	M'_{x2}	M'_{y3}	N'_{y1}	N'_{y2}	N'_{x1}	N'_{x2}	N'_{x3}	N'_{y3}
4	20·78	2·05	31·9	9·88	−62·7	−43·6	0·729	−0·913	−0·347	0	−0·604	0
	41·56	4·13	64·3	20·4	−126	−86·9	3·53	−4·56	−0·936	0	−2·24	0
	63·73	6·33	98·8	32·1	−193	−133	9·25	−12·1	−1·45	0	−4·88	0
	96·98	9·47	148	48·9	−290	−201	22·9	−30·4	−1·50	0	−10·5	0
5	20	1·86	28·6	8·62	−57·9	−42·5	0·262	−0·171	2·31	2·52	−5·76	0·429
	41·56	3·46	52·0	15·5	−112	−90·5	0·690	−0·374	7·18	7·87	−21·1	2·17
	63·73	4·75	70·0	20·8	−160	−141	1·06	−0·466	12·4	13·6	−41·3	5·60
	96·98	6·29	90·3	26·8	−222	−216	1·53	−0·517	19·9	21·9	−74·6	13·5
6	20·78	1·74	26·1	7·88	−55·9	−41·4	2·25	1·88	7·00	7·17	0·017	2·45
	41·56	2·79	40·3	12·0	−97·1	−76·4	6·01	5·29	18·2	18·7	0·024	7·15
	63·73	3·55	49·5	14·7	−133	−109	10·1	9·08	29·8	30·5	0·088	12·8
	96·98	4·39	58·5	17·4	−178	−151	15·8	14·5	45·9	46·8	0·337	21·4
(linear)		2·73	4·23	1·29	−8·33	−5·82						
$36{\cdot}09\frac{l_x^4}{h^4}\cdot\frac{q}{E}=1$		$\times10^{-3}$	$\times10^{-2}$	$\times10^{-2}$	$\times10^{-2}$	$\times10^{-2}$	0	0	0	0	0	0

TABLE 5 Rotationally fixed square plates under uniform transverse pressure and increasing uniaxial end-thrust

Plate	$\frac{l_x^4}{h^4}\cdot\frac{q}{E}$	Applied load N'_x average	W_1	M'_{x1}	M'_{y1}	M'_{x2}	M'_{y3}	N'_{x1}	N'_{y1}	N'_{x2}	N'_{x3}	N'_{x4}	N'_{y3}	Buckling breadth ratio based on strain	Buckling breadth ratio based on stress
7	2	0	0·0943	1·65	1·65	−3·62	−3·62	0·0158	0·0158	0·0066	−0·014	0·0052	0·0066	—	—
		−46	0·176	3·57	3·37	−4·95	−6·28	−45·9	0·061	−46·0	−46·0	−46·0	0·0198	0·999	0·998
		−64	0·269	5·96	5·38	−6·18	−9·36	−63·9	0·154	−63·9	−64·1	−64·0	0·0419	0·999	0·996
		−90	1·01	26·3	21·7	−14·1	−34·6	−87·7	2·47	−89·4	−91·9	−89·3	0·461	0·999	0·980
8	10	0	0·469	8·21	8·21	−18·1	−18·1	0·395	0·395	0·165	−0·354	0·130	0·165	—	—
		−30	0·667	12·7	12·3	−21·5	−24·5	−29·2	0·844	−29·7	−30·7	−29·7	0·306	0·987	0·978
		−70	1·43	31·8	28·4	−31·8	−50·6	−72·8	4·44	−68·7	−73·6	−68·7	1·20	0·974	0·965
		−100	3·02	72·7	59·5	−46·4	−112	−81·2	20·5	−94·4	−117	−93·9	4·71	0·923	0·854

TABLE 6 Rotationally fixed 3/1 rectangular plates under uniform transverse pressure and increasing uniaxial end-thrust

Plate	$\frac{l_x^4}{h^4} \cdot \frac{q}{E}$	Applied load N'_y average	W_1	W at x = 0 y = 0·325 ly	M'_{x1}	M'_{y1}	M'_{x2}	M'_{y3}	N'_{x1}	N'_{y1}	N'_{x2}	N'_{y2}	N'_{y3}	N'_{y4}	Buckling-breadth ratio based on strain	Buckling-breadth ratio based on stress
9	2	0	0·197	0·148	3·05	0·932	−6·01	−4·20	0·0279	0·0036	0·0302	−0·0026	0·0039	0·011	—	—
		−28	0·198	0·171	3·04	0·841	−5·99	−4·22	0·0192	−28·0	0·023	−28·0	−28·0	−28·0	1·00	1·00
		−50	0·182	0·209	2·74	0·555	−5·49	−4·23	−0·0057	−50·0	0·0014	−50·0	−50·0	−50·0	1·00	1·00
		−70	−0·078	0·313	−2·62	−5·29	2·96	−2·74	−0·317	−69·9	−0·137	−70·1	−70·1	−69·4	0·999	0·998
10	10	0	0·969	0·738	15·0	4·55	−29·7	−21·1	0·680	0·086	0·735	−0·061	0·098	0·280	—	—
		−28	0·975	0·853	15·0	4·17	−29·7	−21·2	0·462	−28·0	0·552	−28·0	−27·9	−27·6	0·994	1·00
		−50	0·920	1·02	13·9	3·15	−27·9	−21·3	−0·030	−50·1	0·116	−49·8	−49·9	−49·1	0·994	0·999
		−70	0·551	1·376	6·88	−3·06	−16·3	−20·1	−1·86	−70·2	−1·42	−69·7	−70·3	−66·8	0·993	0·998
11	20	0	1·86	1·46	28·5	8·59	−57·8	−42·6	2·40	0·279	2·61	−0·186	0·420	1·06	—	—
		−28	1·88	1·67	28·8	8·13	−58·0	−43·0	1·73	−27·9	2·02	−28·0	−27·5	−26·4	0·974	0·937
		−50	1·84	1·94	28·1	7·29	−56·5	−43·4	0·626	−50·2	0·988	−49·6	−49·4	−47·3	0·982	0·944
		−60	1·80	2·12	27·3	6·83	−54·8	−43·5	−0·198	−60·4	0·156	−59·4	−59·4	−56·3	0·982	0·940

TABLE 7 Example 3 Rotationally fixed square plates under uniform transverse pressure and uniaxial end-thrust

	Plate	q lb/sq.in.	Average end-thrust σ_{xm} tons/sq.in	Central deflexion w_1 in.	Bending stresses tons/sq. in. σ_{xb1}	σ_{xb2}	σ_{yb3}	Membrane stresses tons/sq. in. σ_{xm1}	σ_{xm2}	σ_{ym2}	σ_{xm3}	Buckling-breadth ratio based on strain	Buckling-breadth ratio based on stress
h = 0·5 in.	7	4·64	−12·28	0·022	±1·79	±2·81	±3·33	−12·26	−12·26	0·005	−12·28	0·999	0·999
	8	23·2	−12·28	0·112	±8·58	±14·0	±16·7	−11·90	−12·15	0·128	−12·55	0·987	0·977
h = 0·35 in.	7	1·11	−11·7	0·035	±2·31	±2·41	±3·47	−11·6	−11·7	0·025	−11·7	0·999	0·998
	8	5·52	−11·7	0·152	±9·53	±9·53	±15·3	−11·0	−11·5	0·020	−12·3	0·974	0·965

TABLE 8 Example 4 Rotationally fixed 3/1 rectangular plates under uniform transverse pressure and uniaxial end-thrust

	Plate	q lb/sq.in.	Average end-thrust σ_{ym} tons/sq.in.	Central deflexion w_1 in.	Deflexion at x = 0 y = 29 in.	Bending stresses tons/ sq.in. σ_{yb1}	σ_{yb3}	σ_{xb2}	σ_{xb1}	Membrane stresses tons/sq. in. σ_{ym1}	σ_{ym3}	σ_{xm2}	σ_{ym2}	Buckling-breadth ratio based on strain	stress
h = 0·5 in.	9	4·64	−12·28	0·030	0·027	±0·475	±2·61	±3·45	±1·83	−12·3	−12·3	0·004	−12·3	1	1
	10	23·2	−12·28	0·145	0·136	±2·41	±13·1	±18·1	±9·10	−12·3	−12·3	0·147	−12·3	0·994	0·999
h = 0·35 in.	9	1·11	−10	0·016	0·026	±0·036	±1·26	±1·40	±0·667	−10·0	−10·0	−0·004	−10·0	1	0·990
	11	11·1	−10	0·189	0·225	±2·07	±13·18	±16·6	±8·29	−10·1	−9·93	−0·026	−9·93	0·980	0·990

TABLE 9 Example 5 Initially deformed rotationally free square plates under end-thrust

	Plate	$\frac{w_{01}}{h}$	Average end-thrust σ_{xm} tons/sq.in.	Total central deflexion w_1 in.	Central bending stresses σ_{xb1} tons/sq. in.	max. and min. surface stresses at centre tons/sq.in. σ_{x1}	σ_{x1}	max. membrane stress σ_{xm3} tons/sq. in.	Buckling-breadth ratio based on strain	stress
h = 0·5 in.	12	0·1	−12·28	0·274	±11·3	−22·3	+0·400	−13·7	0·90	0·92
	13	0·5	−12·28	0·565	±14·3	−21·7	+6·94	−17·2	0·72	0·71
	14	1	−12·28	0·795	±11·63	−18·1	+5·17	−19·6	0·62	0·62

TABLE 10 Initially deformed rotationally free square plates under increasing end-thrust

Plate	$\frac{W_{01}}{h}$	Applied load N'_x average	W_1	M'_{x1}	M'_{y1}	N'_{x1}	N'_{y1}	N'_{x2}	N'_{x3}	N'_{x4}	N'_{y3}	Buckling-breadth ratio based on strain	Buckling-breadth ratio based on stress
12	0·1	−12	0·4735	1·82	1·82	−11·9	0·143	−11·9	−12·1	−12·1	0·135	0·988	0·988
		−24	0·8135	6·12	6·13	−23·3	0·692	−23·3	−24·7	−24·6	0·656	0·973	0·971
		−36	1·812	18·4	18·5	−32·1	3·88	−32·2	−40·1	−39·4	3·76	0·903	0·898
		−38	2·054	21·2	21·4	−33·9	5·01	−33·1	−43·3	−42·4	4·89	0·883	0·877
13	0·5	−12	2·175	6·34	6·35	−9·32	2·46	−9·62	−14·6	−14·2	2·41	0·829	0·822
		−24	2·897	14·6	14·7	−16·6	6·79	−17·2	−31·3	−30·2	6·80	0·774	0·767
		−36	3·730	23·2	23·7	−21·6	13·2	−22·2	−50·2	−48·8	13·7	0·718	0·713
		−38	3·873	24·5	25·2	−22·2	14·4	−22·8	−53·9	−52·1	15·1	0·709	0·705
14	1	−12	3·929	6·79	6·85	−6·64	5·34	−6·46	−17·8	−17·1	5·52	0·679	0·678
		−24	4·587	13·2	13·6	−12·0	11·8	−11·2	−37·1	−35·9	12·6	0·648	0·648
		−36	5·250	18·8	19·8	−16·5	19·0	−14·5	−57·6	−56·4	21·1	0·622	0·625

TABLE 11 Example 6 Initially deformed rotationally fixed square plates under end-thrust

	Plate	$\frac{w_{01}}{h}$	Average end-thrust σ_{xm} tons/sq. in.	Total central deflexion W_1 in.	Bending stresses tons/sq. in. σ_{xb1}	σ_{xb2}	σ_{yb3}	Membrane stresses tons/sq. in. σ_{xm1}	σ_{xm2}	σ_{ym3}	σ_{xm3}	Buckling-breadth ratio based on strain	Buckling-breadth ratio based on stress
h = 0·5 in.	15	0·1	−12·28	0·077	±2·39	±2·98	±3·76	−12·2	−12·2	0·040	−12·3	0·996	0·994
	16	0·5	−12·28	0·359	±8·89	±12·7	±15·5	−10·7	−11·5	0·785	−13·7	0·932	0·896
	17	1	−12·28	0·647	±10·7	±19·6	±22·9	−8·43	−10·2	2·12	−16·4	0·837	0·770
h = 0·35 in.	15	0·1	−11·7	0·109	±4·90	±4·10	±7·00	−11·4	−11·6	0·100	−11·9	0·980	0·980
	16	0·5	−11·7	0·370	±11·4	±13·5	±20·3	−9·10	−10·6	1·17	−14·1	0·891	0·831
	17	1	−11·7	0·572	±11·0	±18·9	±28·6	−7·10	−9·30	2·54	−16·2	0·803	0·722

TABLE 12 Initially deformed rotationally fixed square plates under increasing end-thrust

Plate	$\frac{w_{01}}{h}$	Applied load N'_x average	W_1	M'_{x1}	M'_{y1}	M'_{x2}	M'_{y3}	N'_{x1}	N'_{y1}	N'_{x2}	N'_{x3}	N'_{x4}	N'_{y3}	Buckling-breadth ratio, based on strain	Buckling-breadth ratio, based on stress
15	0·1	−30	0·4617	2·69	2·59	−3·74	−4·37	−29·8	0·169	−29·9	−30·1	−30·0	0·078	0·997	0·995
		−70	1·023	16·2	14·3	−13·6	−23·2	−68·2	1·87	−69·4	−71·5	−69·7	0·613	0·988	0·976
		−90	2·018	42·2	35·1	−25·2	−58·4	−82·2	8·50	−87·6	−96·9	−88·0	2·20	0·962	0·872
		−100	2·717	60·5	48·7	−31·6	−85·6	−85·5	16·0	−95·6	−113·1	−95·9	3·88	0·938	0·885
16	0·5	−30	2·208	10·9	10·6	−16·6	−19·1	−26·6	3·45	−28·3	−33·1	−29·7	1·69	0·938	0·906
		−70	3·490	37·6	34·1	−44·5	−67·0	−54·6	16·3	−63·2	−84·5	−67·6	7·023	0·891	0·830
		−90	4·322	54·7	48·0	−58·5	−102	−63·8	28·2	−78·6	−115	−85·0	11·7	0·861	0·782
		−100	4·739	62·9	54·3	−64·6	−122	−67·3	35·4	−85·8	−132	−93·2	14·6	0·845	0·757
17	1	−30	4·098	14·1	13·7	−26·2	−29·5	−21·1	9·05	−25·2	−38·6	−29·4	4·89	0·843	0·778
		−70	5·396	36·2	34·1	−62·3	−83·8	−42·8	28·2	−55·4	−97·0	−66·5	15·1	0·803	0·722
		−90	6·075	46·6	43·3	−79·2	−116	−51·1	40·6	−68·9	−129	−83·9	22·0	0·784	0·697
		−100	6·419	51·5	47·7	−87·3	−134	−54·8	47·2	−75·3	−146	−92·4	25·8	0·776	0·685

TABLE 13 Initially deformed rotationally fixed 3/1 rectangular plates under increasing end-thrust

Plate	$\frac{w_{01}}{h}$	Applied ave. end-thrust N'_x	Applied ave. end-thrust N'_y	W_1	M'_{x1}	M'_{x2}	M'_{y1}	M'_{y3}	max N'_x at $x = 0$	max N'_x at $x = \frac{lx}{2}$	max N'_y at $y = 0$	max N'_y at $y = \frac{ly}{2}$	Buckling-breadth ratio based on stress: x direction	Buckling-breadth ratio based on stress: y direction
19	0·1	0	−8	0·337	0·105	−0·181	0·038	−0·054	−0·002	0·002	−8·00	−8·00	—	1
		0	−40	0·365	0·563	−0·967	0·196	−0·204	−0·025	0·024	−40·0	−40·0	—	1
		0	−60	0·382	0·835	−1·44	0·242	−0·177	−0·042	−0·038	−60·0	−60·0	—	1
20	0·5	0	−8	1·68	0·497	−0·858	0·174	−0·280	−0·056	0·055	−8·01	−8·00	—	0·999
		0	−40	1·80	2·43	−4·21	0·778	−1·16	−0·592	−0·540	−40·1	−40·0	—	0·998
		0	−60	1·87	3·56	−6·19	0·987	−1·25	−0·963	−0·872	−60·1	−60·0	—	0·998
21	1	0	−8	3·35	0·814	−1·41	0·251	−0·611	−0·224	0·220	−8·05	−8·00	—	0·994
		0	−40	3·54	3·79	−6·60	1·14	−2·88	−2·01	−1·79	−40·2	−40·0	—	0·993
		0	−60	3·65	5·54	−9·72	1·57	−3·89	−3·29	−2·86	−60·2	−60·1	—	0·988
22	0·5	−8	−8	1·99	5·68	−9·14	1·91	−3·44	−9·40	−9·28	−8·24	−7·99	0·851	0·971
		−20	−20	2·78	19·4	−28·1	6·00	−12·7	−26·3	−25·6	−20·8	−20·1	0·760	0·952
		−28	−28	3·56	33·4	−45·0	9·56	−26·5	−42·3	−40·1	−29·0	−28·2	0·662	0·909
23	0·5	−4	−8	1·83	2·92	−4·86	1·00	−1·68	−4·51	−4·47	−8·10	−8·00	0·885	0·988
		−16	−32	2·57	15·6	−23·3	4·71	−9·09	−20·8	−20·3	−32·6	−32·1	0·769	0·982
		−22	−44	3·09	24·7	−34·9	6·71	−16·4	−31·9	−30·4	−44·6	−44·1	0·690	0·954

TABLE 14 Example 7 Initially deformed rotationally fixed 3/1 rectangular plates under end-thrust

	Plate	$\frac{w_{01}}{h}$	Average end-thrust σ_{ym} tons/sq. in.	Total central deflection w_1 in.	Bending stresses tons/sq. in. σ_{xb1}	σ_{bx2}	σ_{yb3}	Membrane stresses tons/sq. in. σ_{xm} max	σ_{ym3}
h = 0·5 in.	19	0·1	−13·6	0·055	±0·348	±0·598	±0·126	−0·009	−13·6
	20	0·5	−13·6	0·272	±1·50	±2·60	±0·717	−0·202	−13·6
	21	1	−13·6	0·535	±2·34	±4·08	±1·78	−0·685	−13·6
h = 0·35 in.	19	0·1	−10	0·040	±0·253	±0·436	±0·054	−0·007	−10·0
	20	0·5	−10	0·198	±1·08	±1·88	±0·379	−0·161	−10·0
	21	1	−10	0·387	±1·68	±2·95	±1·18	−0·549	−10·0

TABLE 15 Example 8 Initially deformed rotationally fixed 3/1 rectangular plates under biaxial end-thrust $\left(\frac{w_{01}}{h} = 0{\cdot}5\right)$

	Plate	Applied ave. end-thrust tons/sq. in. σ_{xm}	σ_{ym}	Total central deflexion w_1 in.	max. bending stresses tons/sq. in. σ_{xb}	σ_{yb}	max. membrane stresses tons/sq. in. σ_{xm}	σ_{ym}	Buckling-breadth ratio based on stress x direction	y direction
h = 0·5 in.	20	0	−15·0	0·245	±2·86	±9·42	−0·078	−15·0	—	0·998
	22	−7·50	−7·50	0·448	±19·8	±9·58	−10·2	−7·95	0·746	0·941
	23	−7·50	−15·00	0·467	±21·6	±10·1	−10·9	−15·2	0·690	0·954
h = 0·5 in.	24	0	−5·46	0·278	±1·14	±0·518	−0·313	−5·46	—	0·994
	25	−2·73	−2·73	0·504	±7·48	±2·00	−5·76	−3·31	0·473	0·823
	26	−2·73	−5·46	0·462	±8·47	±5·98	−6·58	−6·34	0·415	0·860

TABLE 16 Example 8 Initially deformed rotationally free 3/1 rectangular plates under increasing end-thrust

Plate	$\frac{w_{01}}{h}$	Applied ave. end-thrust N'_x	N'_y	W_1	M'_{x1}	M'_{y1}	M'_y max	max N'_x at x = 0	x = $\frac{lx}{2}$	max N'_y at y = 0	y = $\frac{ly}{2}$	Buckling-breadth ratio based on stress x direction	y direction
24	0·5	0	−8	1·75	0·919	0·302	0·370	−0·418	−0·410	−8·03	−8·05	—	0·993
		0	−20	1·89	2·32	0·669	1·13	−1·20	−1·19	−20·1	−20·2	—	0·990
		0	−32	2·03	3·53	0·668	2·87	−2·29	−2·31	−32·0	−32·5	—	0·992
25	0·5	−2	−2	1·90	2·44	0·791	0·987	−3·12	−3·09	−2·10	−2·13	0·960	0·939
		−6	−6	2·52	8·46	2·43	4·25	−11·3	−11·3	−6·26	−6·94	0·531	0·865
		−10	−10	3·34	16·3	4·17	10·9	−23·9	−24·0	−10·3	−13·5	0·417	0·741
26	0·5	−2	−4	1·92	2·69	0·859	1·11	−3·26	−3·23	−4·11	−4·15	0·615	0·964
		−4	−8	2·25	5·82	1·73	2·73	−7·32	−7·28	−8·19	−8·50	0·546	0·941
		−8	−16	3·06	13·6	3·28	9·67	−19·2	−19·3	−16·2	−18·6	0·415	0·860

TABLE 17 Example 9 Initially deformed 3/1 rectangular plates under combined action of end-thrust and transverse pressure

	Plate	$\frac{w_{01}}{h}$	q lb/sq. in.	Applied ave. end-thrust σ_{ym} tons/sq. in.	Central deflexion w_1 in.	Bending stresses tons/sq. in.				Membrane stresses tons/sq. in.				Buckling-breadth ratio, based on	
						σ_{yb1}	σ_{yb3}	σ_{xb1}	σ_{xb2}	σ_{ym1}	σ_{ym3}	σ_{xm2}	σ_{ym2}	stress	strain
h = 0·5 in.	5	0	23·2	0	0·146	±2·81	±13·02	±9·26	±18·37	0·027	0·034	0·244	−0·195	—	—
	10	0	23·2	−12·28	0·145	±2·41	±13·1	±9·10	±18·1	−12·3	−12·3	0·147	−12·3	0·994	0·994
	20	0·5	0	−12·28	0·270	±0·442	±0·663	±1·35	±2·34	−12·3	−12·3	0·153	−12·3	0·998	0·998
	27	0·5	23·2	−12·28	0·394	±2·35	±14·6	±9·01	±18·2	−12·2	−12·1	0·902	−12·4	0·961	0·980
h = 0·35 in.	5	0	5·52	0	0·103	±1·38	±6·39	±4·54	±9·01	0·011	0·017	0·120	−0·010	—	—
	10	0	5.52	−10	0·089	±0·603	±6·43	±3·76	±7·67	−10·0	−10·0	−0·060	−9·95	0·990	0·990
	20	0·5	0	−10	0·198	±0·299	±0·379	±1·08	±1·88	−10·0	−10·0	0·108	−10·0	0·997	0·998
	27	0·5	5·52	−10	0·281	±1·20	±7·55	±4·63	±9·29	−9·99	−9·90	0·336	−10·0	0·961	0·985

TABLE 18 Graded mesh

Mesh No.	Mesh lengths are given from the centre to the side as ratios of the average mesh length	
No. 1 12 × 20	along x—x	1·125, 1·125, 1·125, 1·125, 1, 0·5
	along y—y	1·5, 1·5, 1·5, 1, 1, 1, 1, 0·5, 0·5, 0·5
No. 2 12 × 20	along x—x	uniform
	along y—y	1·5, 1·5, 1·5, 1, 1, 1, 1, 0·5, 0·5, 0·5
No. 3 12 × 12	along both axes	1·125, 1·125, 1·125, 1·125, 1, 0·5

PRINTED BY Unwin Brothers Limited
THE GRESHAM PRESS OLD WOKING SURREY ENGLAND

Produced by 'Uneoprint'

A member of the Staples Printing Group (UO9383)